SCIENCE CHINA
Information Sciences

• RESEARCH PAPER •

April 2022, Vol. 65 142201:1–142201:13
https://doi.org/10.1007/s11432-020-3121-3

New design of active disturbance rejection control for nonlinear uncertain systems with unknown control input gain

Sen CHEN[1], Zhixiang CHEN[2], Yi HUANG[3,4] & Zhi-Liang ZHAO[1*]

[1]*School of Mathematics and Statistics, Shaanxi Normal University, Xi'an* 710119*, China;*
[2]*Department of Missile Launching and Power, Rocket Force Sergeant Academy, Weifang* 262500*, China;*
[3]*Key Laboratory of Systems and Control, Academy of Mathematics and Systems Science, Chinese Academy of Sciences, Beijing* 100190*, China;*
[4]*School of Mathematical Sciences, University of Chinese Academy of Sciences, Beijing* 100049*, China*

Received 6 August 2020/Revised 9 October 2020/Accepted 30 October 2020/Published online 16 December 2021

Abstract The paper considers the control problem for uncertain nonlinear systems with unknown control input gain. Based on the information of control direction rather than the nominal value of control input gain, a new active disturbance rejection control design is proposed. In the proposed design, the extended state observer (ESO) is constructed to estimate the total disturbance containing the uncertainty of control input. Via the estimations from ESO, the control input is generated by a designed dynamical system, which can force the actual input to track the ideal input. Moreover, for a wide class of nonlinear uncertainties, the transient performance of the proposed design is investigated. The theoretical results show that the tracking and estimating errors, as well as the difference between the actual and ideal inputs, can be sufficiently small by tuning the parameter of ESO despite various uncertainties. The experiment of a permanent magnet linear synchronous motor servo system illustrates the effectiveness of the proposed design.

Keywords uncertain system, active disturbance rejection control, control input gain

Citation Chen S, Chen Z X, Huang Y, et al. New design of active disturbance rejection control for nonlinear uncertain systems with unknown control input gain. Sci China Inf Sci, 2022, 65(4): 142201, https://doi.org/10.1007/s11432-020-3121-3

1 Introduction

How to tackle the uncertainties is a central issue in control science and technology [1]. To ensure the normal operation of systems against uncertainties, numerous control strategies have been substantially developed, such as proportional-integral-derivative (PID) control [2], robust control [3], sliding-mode control [4], and various disturbance rejection methods [5–8]. Among various disturbance rejection methods, the active disturbance rejection control (ADRC), proposed by Han [8], has drawn much attention from both researchers and practitioners owing to its uniqueness in concepts, simplicity in engineering implementation, and superior performance in practice.

The fundamental idea of ADRC is to actively estimate and compensate for the total disturbance. In the frame of ADRC, the integrator chain describes the internal relationship from the control input to the controlled output. Based on this essential form, the total effects from the internal and external disturbances to the controlled output can be obtained, which generates the concept of uncertainties to the "total disturbance" [9]. Then the extended state observer (ESO) is innovatively constructed to estimate the total disturbance and the derivatives of the controlled output. Via the estimations from ESO, the control input containing the compensation for the total disturbance can be designed. Owing to the effective estimation and compensation for total disturbance, ADRC has been successfully applied to various industrial processes, such as flight systems [10, 11], robotic systems [12], motion

* Corresponding author (email: zhiliangzhao@snnu.edu.cn)

control systems [13, 14], ship control systems [15], tank gun control systems [16] and process control systems [17, 18].

The theoretical foundation of ADRC has been investigated in the last decade. Based on the assumption that the derivative of the total disturbance is bounded, Ref. [19] rigorously analyzed the estimating error of the linear ESO. Besides, the convergence of the nonlinear ESO was investigated in [20] also with the assumption that the derivative of total disturbance is bounded. In [21], by assuming that the derivative of the total disturbance is bounded, the stability of the ADRC-based closed-loop system was proved. Because the total disturbance might be a function dependent on the system states in practice, the derivative of the total disturbance will be influenced by the system state which cannot be assumed to be bounded before designing the controller. Several profound theoretical results of ADRC with the more practical assumptions for total disturbance have been made in [9, 22–26]. In [22], by considering the uncertainties as a linear function of system states with unknown coefficients, the stability region of the unknown linear coefficients was investigated. Ref. [23] revealed that both the tracking and estimating errors can be sufficiently small by suitably tuning the parameter of ESO despite a wide scope of uncertainties with nonlinear growth. Under the certain condition for the initial value, Ref. [24] proved the convergence of the linear ADRC-based closed-loop system for nonlinear uncertainties. For nonlinear ADRC-based closed-loop systems with nonlinear uncertainties, Ref. [25] provided the tunable upper bounds of tracking and estimating errors, which illustrates the stability of nonlinear ADRC design. Moreover, the capability of ADRC for systems not in the form of integrator chain was investigated in [9, 26], which reveals the universality of ADRC design for nonlinear uncertain systems. However, these studies considered the ADRC design with a known nominal control input gain. Besides, the restricts for the difference between the nominal and real control input gains were needed in [9, 23, 26]. More importantly, a recent paper [27] proposed a necessary condition for the nominal control input gain in ADRC, which illuminates the limits of the conventional ADRC to handle uncertain control input gain. Thus, the following question is risen:

Can we improve the capability of ADRC to deal with the uncertain control input gain via some innovative design?

Motivated by this question, the paper investigates the ADRC design for nonlinear uncertain systems with unknown control input gain. Refs. [28–30] innovatively proposed a dynamic inversion-based method to handle the non-affine uncertainties. The key ideology of the dynamic inversion-based method is to design a dynamical system such that the actual control input can track the desired input. Inspired by this innovative design, the paper proposes a new ADRC composed of an ESO and a dynamical system for control input. The ESO is designed to estimate the total disturbance containing the unknown term of control input. Based on the estimations from ESO and the control direction, a dynamical system is constructed to generate the control input, which can force the actual control input to track the ideal control input. Different from the convergence analysis with respect to the observer's parameters in [28–30], the paper rigorously studies the transient performance of the proposed ADRC-based closed-loop system. Moreover, the relationship between the closed-loop performance and the controller parameters is explicitly shown, which further provides a simplified tuning law of the proposed ADRC. Via the simulation of a single-link robotic manipulator system and the experiment of a permanent magnet linear synchronous motor servo system, the effectiveness of the proposed ADRC is illustrated. The main contributions of the paper are presented as follows.

(1) Based on the control direction rather than the nominal control input gain, a new ADRC for nonlinear uncertain systems with unknown control input gain is proposed.

(2) The transient performance of the proposed ADRC-based closed-loop system with a wide class of nonlinear uncertainties is analyzed. Via establishing the relationship between the parameter of ESO and the parameter in dynamical input design, the tracking and estimating errors, as well as the difference between the actual and ideal control inputs, can be sufficiently small despite a wide class of uncertainties by just tuning the parameter of ESO.

The rest of this paper has the following organization. In Section 2, the problem formulation is presented. In Section 3, a new ADRC design based on the information of the control direction is proposed. The transient performance of the proposed ADRC-based closed-loop system is given in Section 4. The simulation and experimental verification are provided in Section 5. Finally, the conclusion is given in Section 6.

Notations. The following notations are used throughout this paper. For a given function $y(t)$, $y^{(k)}(t)$ represents the k-th order derivative of $y(t)$ with respect to the variable t for $k \geqslant 1$ and $y^{(0)}(t) \triangleq y(t)$. $|\cdot|$ and $\|\cdot\|$ are the absolute values of a scalar and the 2-norm of a vector or a matrix, respectively.

For a given matrix or vector A, the corresponding transposition is denoted by A^{T}. $\mathbb{R}$ represents the real number field. The function $\mathrm{sgn}(\cdot)$ is defined as follows:

$$\mathrm{sgn}(a)=\begin{cases}1, & \text{if } a>0,\\ 0, & \text{if } a=0,\\ -1, & \text{if } a<0.\end{cases}$$

2 Problem formulation

Consider the following nonlinear uncertain system:

$$\dot{x}(t)=Ax(t)+B(b(x(t),t)u(t)+f(x(t),t)),\quad y(t)=C^{\mathrm{T}}x(t),\quad t\geqslant t_0, \tag{1}$$

where $x(t)=[x_1(t)\ x_2(t)\ \cdots\ x_n(t)]^{\mathrm{T}}\in\mathbb{R}^n$ is the state vector, $x_i(t)\in\mathbb{R}$ represents the i-th component of the state vector $x(t)$, $y(t)\in\mathbb{R}$ is the measured output to be controlled, $u(t)\in\mathbb{R}$ is the control input, $b(\cdot)\in\mathbb{R}$ represents the control input gain and $f(\cdot)\in\mathbb{R}$ represents the uncertainties including nonlinear uncertain internal dynamics and external disturbances. Additionally, t_0 is the initial time. The matrices A, B, and C have the following forms:

$$A=\begin{bmatrix}0 & 1 & \cdots & 0\\ \vdots & 0 & \ddots & \vdots\\ \vdots & \vdots & \ddots & 1\\ 0 & 0 & \cdots & 0\end{bmatrix}_{n\times n},\quad B=\begin{bmatrix}0\\ \vdots\\ 0\\ 1\end{bmatrix}_{n\times 1},\quad C=\begin{bmatrix}1\\ 0\\ \vdots\\ 0\end{bmatrix}_{n\times 1}. \tag{2}$$

The paper considers the case that only the control direction $\mathrm{sgn}(b)$ is known, where $\mathrm{sgn}(\cdot)$ represents the sign function. The detailed expression of the control input gain $b(\cdot)$, as well as the nominal value of $b(\cdot)$, is unknown.

The control objective is to design the control input $u(t)$ based on the known control direction $\mathrm{sgn}(b)$ such that the output $y(t)$ can track the reference signal $r(t)$. The reference signal satisfies the following assumption.

Assumption 1. There exists a positive constant M_r such that $\sup_{t\geqslant t_0}|r^{(i)}(t)|\leqslant M_r$ for $0\leqslant i\leqslant n+1$.

We assume that the control input gain $b(\cdot)$ and the uncertainties $f(\cdot)$ satisfy the following assumption.

Assumption 2. The functions $b(x,t)$ and $f(x,t)$ are differentiable. There exist continuous functions ψ_f, $\psi_{\bar{b}}$ and $\psi_{\underline{b}}$ such that

$$\sup_{t\geqslant t_0}\left\{|f(x,t)|,\left\|\frac{\partial f(x,t)}{\partial x}\right\|,\left|\frac{\partial f(x,t)}{\partial t}\right|\right\}\leqslant\psi_f(x),\quad\forall x\in\mathbb{R}^n, \tag{3}$$

$$\sup_{t\geqslant t_0}\left\{|b(x,t)|,\left\|\frac{\partial b(x,t)}{\partial x}\right\|,\left|\frac{\partial b(x,t)}{\partial t}\right|\right\}\leqslant\psi_{\bar{b}}(x),\quad\inf_{t\geqslant t_0}|b(x,t)|\geqslant\psi_{\underline{b}}(x)>0,\quad\forall x\in\mathbb{R}^n. \tag{4}$$

Assumption 1 implies that the reference signal and its derivatives are bounded, which is satisfied for practical systems. For Assumption 2, inequalities (3) and (4) illustrate that the functions $b(\cdot)$ and $f(\cdot)$ and their partial derivatives are bounded when the system states stay in a bounded set. Moreover, the inequality (4) illustrates that the lower bound of $|b(\cdot)|$ is larger than zero if the states stay in a bounded set, which is a common assumption also provided in [23,26]. Hence it can be deduced from (4) that the control direction $\mathrm{sgn}(b)$ will not change for various (x,t), which is consistent with the physical mechanism in many practical plants [12,18]. Assumption 2 describes a large scope of nonlinear uncertainties in practice.

Remark 1. Via investigating the relationship between the original system states and the new states composed of the derivatives of the controlled output, a wide class of nonlinear uncertain systems can be transformed into the form (1), including uncertain systems with mismatched uncertainties or measurement uncertainties [9,26]. The detailed analysis technique can be found in [9,26] and is omitted here.

3 New ADRC design

In this section, an ADRC design just based on the information of the control direction is proposed.

3.1 ESO design

In this subsection, an ESO is presented to estimate the system states and the total disturbance.

Because the control input gain $b(\cdot)$ and nonlinearity $f(\cdot)$ are unknown, we define the new state $x_{n+1}(t) \triangleq b(x(t),t)u(t) + f(x(t),t)$. The system (1) can be rewritten as

$$\dot{x}_e(t) = A_e x_e(t) + B_f \dot{x}_{n+1}(t), \quad y(t) = C_{\mathrm{e}}^{\mathrm{T}} x_e(t), \tag{5}$$

where $x_e(t) = [x^{\mathrm{T}}(t)\ x_{n+1}(t)]^{\mathrm{T}} \in \mathbb{R}^{n+1}$ is the extended state vector and the matrices $A_e, B_f,$ and C_e have the following form:

$$A_e = \begin{bmatrix} A & B \\ 0 & 0 \end{bmatrix}_{(n+1)\times(n+1)}, \quad B_f = \begin{bmatrix} 0 \\ \vdots \\ 0 \\ 1 \end{bmatrix}_{(n+1)\times 1}, \quad C_e = \begin{bmatrix} C \\ 0 \end{bmatrix}_{(n+1)\times 1}. \tag{6}$$

For system (5), the following ESO is presented to estimate the extended state vector:

$$\dot{\hat{x}}_e(t) = A_e \hat{x}_e(t) + L_e(y(t) - C_{\mathrm{e}}^{\mathrm{T}} \hat{x}_e(t)), \tag{7}$$

where $\hat{x}_e(t) = [\hat{x}^{\mathrm{T}}(t)\ \hat{x}_{n+1}(t)]^{\mathrm{T}} \in \mathbb{R}^{n+1}$ is the estimation for the extended state vector $x_e(t)$, $\hat{x}(t) = [\hat{x}_1(t)\ \cdots\ \hat{x}_n(t)]^{\mathrm{T}} \in \mathbb{R}^n$ is the estimation for the system state vector $x(t)$ and $\hat{x}_i(t) \in \mathbb{R}$ represents the i-th component of the vector $\hat{x}(t)$. Besides, the parameter vector of ESO $L_e \in \mathbb{R}^{(n+1)\times 1}$ is designed such that the matrix $A_L \triangleq A_e - L_e C_{\mathrm{e}}^{\mathrm{T}}$ is Hurwitz. Ref. [31] proposed an effective simplified tuning method of ESO's parameter vector L_e:

$$L_e = \left[\phi_1\omega_o\ \phi_2\omega_o^2\ \cdots\ \phi_{n+1}\omega_o^{n+1}\right]^{\mathrm{T}}, \quad \phi_i = \frac{(n+1)!}{(n+1-i)!i!}, \quad \omega_o \geqslant 0, \tag{8}$$

such that all the eigenvalues of A_L are set at $-\omega_o$.

3.2 Dynamical design of ADRC input

In this subsection, the ADRC input based on the estimations from ESO is proposed.

Firstly, the ideal trajectory and ideal control input are designed. The ideal trajectory is presented as follows:

$$\dot{x}^*(t) = Ax^*(t) - BK^{\mathrm{T}}(x^*(t) - \bar{r}(t)) + Br^{(n)}(t), \quad y^*(t) = C^{\mathrm{T}}x^*(t), \quad t \geqslant t_0, \quad x^*(t_0) = x(t_0), \tag{9}$$

where $x^*(t) = [x_1^*(t)\ \cdots\ x_n^*(t)] \in \mathbb{R}^n$ is the ideal state vector, $y^*(t) \in \mathbb{R}$ is the ideal output, $\bar{r}(t) = [r(t)\ r^{(1)}(t)\ \cdots\ r^{(n-1)}(t)]^{\mathrm{T}} \in \mathbb{R}^n$ and the constant vector $K \in \mathbb{R}^n$ is designed such that the matrix $A_K \triangleq A - BK^{\mathrm{T}}$ is Hurwitz. The ideal output $y^*(t)$ can exponentially converge to the reference signal $r(t)$.

Owing to the system (1) and the ideal trajectory (9), the ideal control input should be designed as

$$u^*(t) = \frac{-f(x,t) - K^{\mathrm{T}}(x(t) - \bar{r}(t)) + r^{(n)}(t)}{b(x,t)}. \tag{10}$$

Then we consider the ADRC input design based on the estimations from the ESO (7) and the ideal control input (10). The design ideology is to design the control input satisfying the following dynamics:

$$\dot{u}(t) = -a(x,t)(u(t) - u^*(t)), \tag{11}$$

where $a(x,t) > 0$ is a function to be designed. Then the following equation can be obtained based on (10) and (11):

$$\begin{aligned} \dot{u}(t) &= -\frac{a(x,t)}{b(x,t)}(b(x,t)u(t) - b(x,t)u^*(t)) \\ &= -\frac{a(x,t)}{b(x,t)}(x_{n+1}(t) + K^{\mathrm{T}}(x(t) - \bar{r}(t)) - r^{(n)}(t)). \end{aligned} \tag{12}$$

By designing $a(x,t) = |b(x,t)|\lambda(\omega_o)$ and substituting the estimations from ESO into (12), the ADRC input can be designed as follows:

$$\dot{u}(t) = -\mathrm{sgn}(b)\lambda(\omega_o)(\hat{x}_{n+1}(t) + K^{\mathrm{T}}(\hat{x}(t) - \bar{r}(t)) - r^{(n)}(t)), \tag{13}$$

where $\lambda(\omega_o)$ is a function satisfying the following assumption.

Assumption 3. The increasing function $\lambda(\omega_o) > 0$ for $\omega_o > 0$ and

$$\lim_{\omega_o\to\infty} \frac{\ln \omega_o}{\sqrt{\lambda(\omega_o)}} = 0, \quad \lim_{\omega_o\to\infty} \frac{\omega_o}{\lambda(\omega_o)} = \infty. \tag{14}$$

Remark 2. The function $\lambda(\omega_o) = \omega_o^k$ with $0 < k < 1$ can satisfy Assumption 3. Based on the specific expression of $\lambda(\omega_o)$, the proposed ADRC has the same number of the adjustable parameters as the conventional ADRC, i.e., ω_o and K.

Remark 3. If u^* is a constant and the signal $u(t)$ satisfies the following dynamics:

$$\dot{u}(t) = -a(u(t) - u^*), \quad t \geqslant t_0 \tag{15}$$

for a constant $a > 0$, then it can be deduced that $u(t) = \mathrm{e}^{-at}u(t_0) + (1 - \mathrm{e}^{-a(t-t_0)})u^*$. Hence $u(t)$ can exponentially converge to u^* with the desired convergence rate determined by a.

Finally, a new design of ADRC is proposed, i.e., (7) and (13). It is significant to point out that the proposed design just requires the sign of the control input gain $b(\cdot)$ rather than the detailed value or the functional structure of $b(\cdot)$.

In Section 4, the transient performance of the proposed ADRC is analyzed.

4 Performance analysis

The following theorem illuminates the transient performance of the proposed design.

Theorem 1. Consider the system (1) with Assumptions 1–3. Let $u(t) = 0$ for $t \in [t_0, t_u)$ where

$$\begin{cases} t_u = t_0 + 2nc_{\phi 2}\dfrac{\max\{\ln(\omega_o\rho_0),\ 0\}}{\sqrt{\lambda(\omega_o)}}, \quad \rho_0 = \max\limits_{2\leqslant i\leqslant n} |x_i(t_0) - \hat{x}_i(t_0)|^{\frac{1}{n}}, \\ c_{\phi 2} = \lambda_{\max}(P_\phi), \quad A_\phi^{\mathrm{T}}P_\phi + P_\phi A_\phi = -I, \quad A_\phi = \begin{bmatrix} -\phi_1 & 1 & 0 & \cdots & 0 \\ \vdots & & \ddots & \ddots & \vdots \\ \vdots & 0 & \ddots & \ddots & 0 \\ \vdots & \vdots & \ddots & \ddots & 1 \\ -\phi_n & 0 & \cdots & 0 & 1 \\ -\phi_{n+1} & 0 & \cdots & \cdots & 0 \end{bmatrix}. \end{cases} \tag{16}$$

For $t \geqslant t_u$, $u(t)$ is designed according to (7) and (13). Then there exist positives η_i^* $(1 \leqslant i \leqslant 5)$ and ω^* dependent on $(x_e(t_0), \hat{x}_e(t_0), \psi_f, \psi_{\bar{b}}, \psi_{\underline{b}}, M_r, K)$ such that

$$\sup_{t\geqslant t_0} \|x(t) - x^*(t)\| \leqslant \eta_1^* \max\left\{\frac{\ln\omega_o}{\sqrt{\lambda(\omega_o)}}, \frac{\lambda(\omega_o)}{\omega_o}, \frac{1}{\lambda(\omega_o)}\right\}, \tag{17}$$

$$\|x_e(t) - \hat{x}_e(t)\| \leqslant \eta_2^*\left(\frac{\lambda(\omega_o)}{\omega_o} + \mathrm{e}^{-\eta_3^*\omega_o(t-t_u)}\right), \quad \forall t \geqslant t_u, \tag{18}$$

$$|u(t) - u^*(t)| \leqslant \eta_4^*\left(\frac{\lambda(\omega_o)}{\omega_o} + \frac{1}{\lambda(\omega_o)} + \mathrm{e}^{-\eta_5^*\lambda(\omega_o)(t-t_u)}\right), \quad \forall t \geqslant t_u, \tag{19}$$

for any $\omega_o \geqslant \omega^*$.

From Theorem 1, the bounds of tracking and estimating errors, as well as the difference between the actual and ideal control inputs, are provided. According to the tuning law of $\lambda(\omega_o)$ shown in Assumption 3, Eq. (17) implies that the actual trajectory $x(t)$ can approach the ideal one $x^*(t)$ by tuning ω_o to be suitably large. Moreover, the satisfied estimating performance of ESO is illustrated by (18). As shown in (19), the difference between the actual control input $u(t)$ and the ideal input $u^*(t)$ can be sufficiently small via adjusting ω_o.

The proof of Theorem 1 is given in Appendix A.

Remark 4. The design of t_u is to prevent from the poor closed-loop performance caused by the peaking phenomenon of ESO, which is a common method as shown in [9,23,26]. Moreover, if the initial condition satisfies that $\max_{2\leqslant i\leqslant n}|x_i(t_0)-\hat{x}_i(t_0)|^{\frac{1}{n}}\leqslant\frac{1}{\omega_o}$, then $t_u=t_0$ and the satisfied transient performance (17)–(19) can be obtained by designing $u(t)$ as (7) and (13) for $t\geqslant t_0$.

5 Simulations and experiments

5.1 Application example: single-link robotic manipulator

In this subsection, the simulations of a robotic manipulator system are presented.

Consider the following single-link robotic manipulator coupled to a direct current (DC) motor with a nonrigid joint [32]:

$$\begin{cases} J_1\ddot{q}_1(t)+F_1\dot{q}_1(t)+K\left(q_1(t)-\dfrac{q_2(t)}{N}\right)+mgd\cos(q_1(t))=0,\\ J_2\ddot{q}_2(t)+F_2\dot{q}_2(t)-\dfrac{K}{N}\left(q_1(t)-\dfrac{q_2(t)}{N}\right)=K_ti(t),\\ L\dot{i}(t)+Ri(t)+K_b\dot{q}_2(t)=u(t)+f_N(q_1,\dot{q}_1,q_2,\dot{q}_2,i), \end{cases} \tag{20}$$

where $q_1(t)\in\mathbb{R}$ and $q_2(t)\in\mathbb{R}$ are the angular positions of the link and the motor shaft at time t, $i(t)\in\mathbb{R}$ is the armature current, and $u(t)\in\mathbb{R}$ is the armature voltage. The inertias J_1 and J_2, the viscous friction coefficients F_1 and F_2, the spring coefficient K, the torque coefficient K_t, the back electromotive force (EMF) coefficient K_b, the armature resistance R, the armature inductance L, the link mass m, the position of the link's center of gravity d, the gear ratio N and the acceleration of gravity g are constants. The function $f_N(\cdot)$ represents the unmodeled dynamics for DC motor.

Based on the measurement of the angular position of the link $q_1(t)$, the control objective is to design the armature voltage $u(t)$ such that $q_1(t)$ can track the reference signal $r(t)$ despite the unknown system parameters $(J_1,J_2,F_1,F_2,K,K_t,K_b,R,L,N,m,d,\mathrm{g})$ and uncertainty f_N.

By defining the following new states:

$$\begin{cases} x_1=q_1,\\ x_2=\dot{q}_1,\\ x_3=\left(-F_1\dot{q}_1(t)-K\left(q_1(t)-\dfrac{q_2}{N}\right)-mgd\cos(q_1(t))\right)/J_1,\\ x_4=\left(-F_1x_3-K\dot{q}_1+\dfrac{K\dot{q}_2}{N}-mgd\dfrac{\mathrm{d}(\cos(q_1(t)))}{\mathrm{d}t}\right)/J_1,\\ x_5=\left(-F_1x_4-Kx_3-\dfrac{KF_2\dot{q}_2}{NJ_2}+\dfrac{K^2}{N^2J_2}\left(x_1-\dfrac{q_2}{N}\right)+\dfrac{K_tKi}{NJ_2}-mgd\dfrac{\mathrm{d}^2(\cos(q_1))}{\mathrm{d}t^2}\right)/J_1, \end{cases} \tag{21}$$

the single-link robotic manipulator system (20) can be rewritten as (1) with $b=\frac{K_tK}{NLJ_1J_2}$ and $f=\frac{K_tKRi}{NLJ_2}-\frac{K_tKK_b\dot{q}_2}{L}-\frac{F_1x_5}{J_1}-\frac{Kx_4}{J_1}-\frac{KF_2}{NJ_1J_2}\ddot{q}_2+\frac{K^2x_2}{N^2J_2}-\frac{K^2\ddot{q}_2}{N^2J_1J_2}-\frac{mgd}{J_1}\frac{\mathrm{d}^3\cos(q_1)}{\mathrm{d}t^3}+f_N$. Although the detailed values of the system parameters $(J_1,J_2,F_1,F_2,K,K_t,K_b,R,L,N,m,d,\mathrm{g})$ are unknown, the control direction satisfies that $b>0$ based on the physical mechanism.

To verify the capability of handling uncertainties, the following f_N, containing step disturbance, sinusoidal disturbance and unknown internal uncertainty, is tested in simulations:

$$f_N=\begin{cases} 0, & \text{if } 0\leqslant t<5,\\ 80, & \text{if } 5\leqslant t<10,\\ 50\sin(t), & \text{if } 10\leqslant t<15,\\ 3(q_1+\dot{q}_1+q_2+\dot{q}_2+i), & \text{if } t\geqslant 15. \end{cases} \tag{22}$$

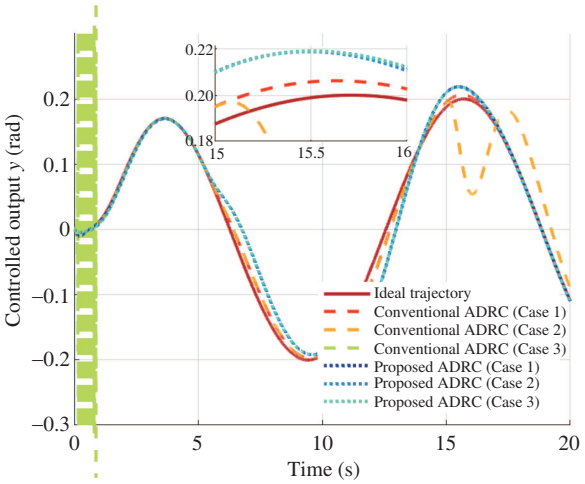

Figure 1 (Color online) The tracking performance of proposed ADRC and conventional ADRC for Cases 1–3.

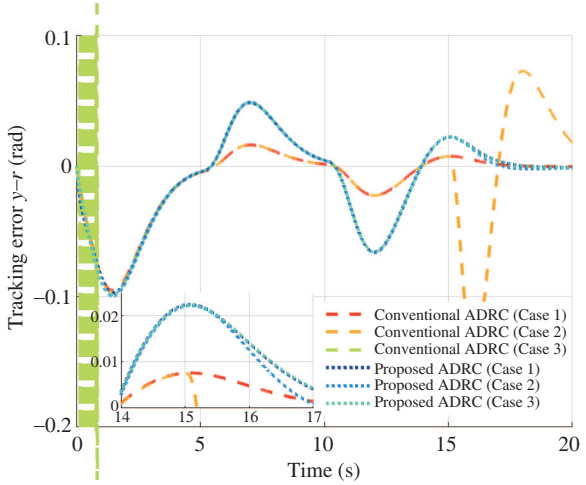

Figure 2 (Color online) The tracking errors of proposed ADRC and conventional ADRC for Cases 1–3.

Moreover, the following groups of system parameters are considered:

$$\begin{cases} \text{Case 1: } J_1 = J_2 = F_1 = F_2 = K = K_t = K_b = R = L = N = 1, \quad m = d = \dfrac{1}{2}, \quad \mathrm{g} = 10, \\ \text{Case 2: } J_1 = J_2 = K_t = L = N = 1, \quad F_1 = F_2 = R = K = K_b = 2, \quad K_t = 1.22, \quad m = d = \dfrac{1}{2}, \quad \mathrm{g} = 10, \\ \text{Case 3: } F_1 = F_2 = K = K_t = K_b = R = L = N = 1, \quad J_1 = J_2 = m = d = \dfrac{1}{2}, \quad \mathrm{g} = 10. \end{cases}$$

Then the proposed ADRC (7) and (13) is designed with ϕ_i satisfying (8), $\omega_o = 400$, $\lambda = \sqrt{\omega_o}$ and $K = [32\ 80\ 80\ 40\ 10]^{\mathrm{T}}$. Besides, the following conventional ADRC with the same (ϕ_i, ω_o, K) is considered in simulations:

$$\begin{cases} \hat{x}_i(t) = \hat{x}_{i+1}(t) + \phi_i \omega_o^i (y(t) - \hat{x}_1(t)), \quad i = 1, 2, 3, 4, \\ \hat{x}_5(t) = \hat{x}_6(t) + b_u u(t) + \phi_5 \omega_o^5 (y(t) - \hat{x}_1(t)), \\ \hat{x}_6(t) = \phi_6 \omega_o^6 (y(t) - \hat{x}_1(t)), \\ u(t) = \dfrac{-\hat{x}_6(t) - K^{\mathrm{T}}([\hat{x}_1(t)\ \cdots\ \hat{x}_5(t)]^{\mathrm{T}} - \bar{r}(t)) + r^{(5)}(t)}{b_u}. \end{cases} \tag{23}$$

The nominal value of input gain b_u is selected as 1, which is the real value of b in Case 1.

Let the reference signal $r(t) = 0.2\sin(t/2)$. The simulation results are shown in Figures 1 and 2. From Figures 1 and 2, when b_u is equal to the real value of b (Case 1), the conventional ADRC-based closed-loop system has better tracking performance. However, when the control input gain b varies owing to the varieties of the system parameters (Cases 2 and 3), the tracking performance of the conventional ADRC-based closed-loop system becomes poor. In Case 3, the real value of control input gain $b = 4$ which exceeds the limits of conventional ADRC to handle the uncertain control input gain [27]. Hence the conventional ADRC-based closed-loop system becomes unstable for Case 3. Moreover, Figures 1 and 2 show that the proposed ADRC still achieves satisfied tracking performance for Cases 2 and 3, which illustrates that the proposed ADRC has the stronger robustness to the uncertainty of control input gain.

5.2 Experiment verification: permanent magnet linear synchronous motor servo system

In this subsection, the experiments of a permanent magnet linear synchronous motor (PMLSM) servo system are presented.

The PMLSM servo system can be modeled as follows [33]:

$$\dot{x}_1(t) = x_2(t), \quad \dot{x}_2(t) = \frac{k_f}{m} u(t) - \frac{B}{m} x_2(t) + \frac{f_s}{m} + \frac{f_l}{m}, \tag{24}$$

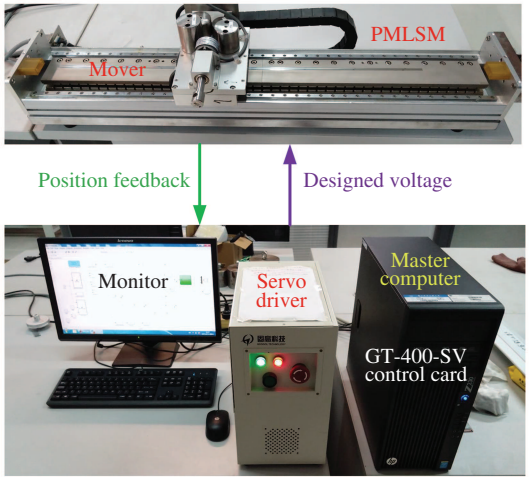

Figure 3 (Color online) Experimental setup of PMLSM servo system.

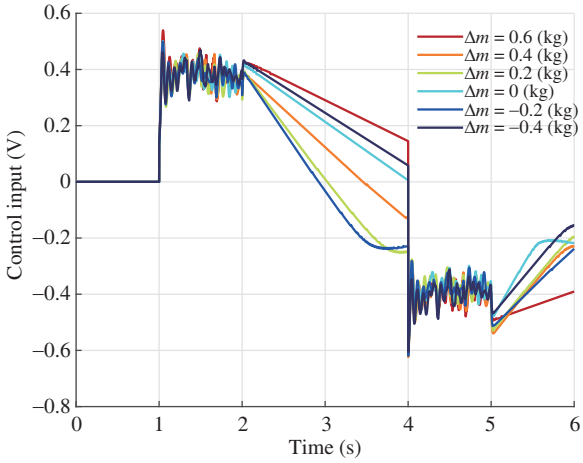

Figure 4 (Color online) The control inputs of proposed ADRC for various load masses (26).

where $x_1(t) \in \mathbb{R}$ is the position of the mover, $x_2(t) \in \mathbb{R}$ is the velocity of the mover, $u(t) \in \mathbb{R}$ is the voltage, and the constants m, B, and k_f are the mass of the mover, the viscous coefficient and the thrust coefficient, respectively. f_s and f_l represent the unknown Coulomb moving friction force and external load force, respectively.

Based on the measurement of the position of the mover $x_1(t)$, the control objective is to design the voltage $u(t)$ such that $x_1(t)$ can track the reference signal $r(t)$.

Let $b = \frac{k_f}{m}$ and $f = -\frac{B}{m}x_2 + \frac{f_s}{m} + \frac{f_l}{m}$. Although the system parameters m, B, and k_f and the dynamics f_s and f_l are unknown, the control direction satisfies that $b > 0$ owing to the physical mechanism. Hence the proposed ADRC (7) and (13) can be designed. The control parameters are chosen as $\omega_o = 256,\ \lambda = \sqrt{\omega_o} = 16,\ K = [625\ 50]^{\mathrm{T}},\ \phi_1 = \phi_2 = 3,\ \phi_3 = 1$. The following reference signal is considered:

$$r(t) = \begin{cases} 0, & \text{if } 0 \leqslant t < 1, \\ 0.1t - 0.1, & \text{if } 1 \leqslant t < 2, \\ 0.1, & \text{if } 2 \leqslant t < 4, \\ -0.1t + 0.5, & \text{if } 4 \leqslant t < 5, \\ 0, & \text{if } t \geqslant 5. \end{cases} \tag{25}$$

To verify the robustness of the proposed design to uncertainties, the following varieties of the load mass are considered in the experiment:

$$\Delta m \in \{-0.4\ (\mathrm{kg}),\ -0.2\ (\mathrm{kg}),\ 0\ (\mathrm{kg}),\ 0.2\ (\mathrm{kg}),\ 0.4\ (\mathrm{kg}),\ 0.6\ (\mathrm{kg})\}. \tag{26}$$

The experimental setup is shown in Figure 3. Via the encoder (type: MicroE 126-70012-c), the position of the mover is acquired and transmitted to the master computer. With the designed control algorithm in the master computer, the digital control input is generated. The control card (type: GT-400-VS) is employed as a real-time controller.

The experimental results are presented in Figures 4–6. From Figures 5 and 6, the closed-loop performance of the proposed ADRC is highly consistent with each other despite the perturbations of the load mass. For various load masses, the control inputs change smoothly, as shown in Figure 4. The experimental results illustrate the effectiveness of the proposed ADRC for uncertain systems with unknown control input gain.

6 Conclusion

The control problem for nonlinear uncertain systems with unknown control input gain is considered. A new ADRC design is proposed, which only requires the information of control direction. The ESO is

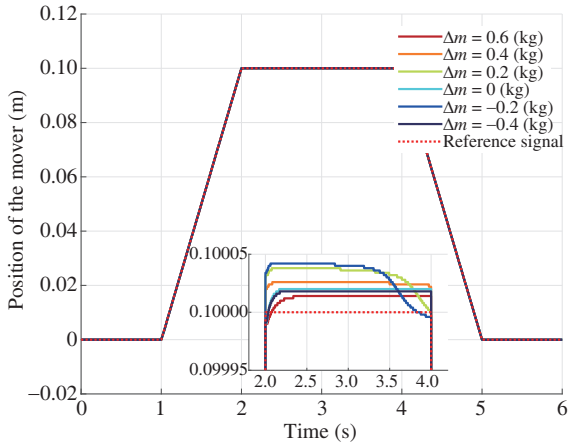

Figure 5 (Color online) The positions of the mover for various load masses (26).

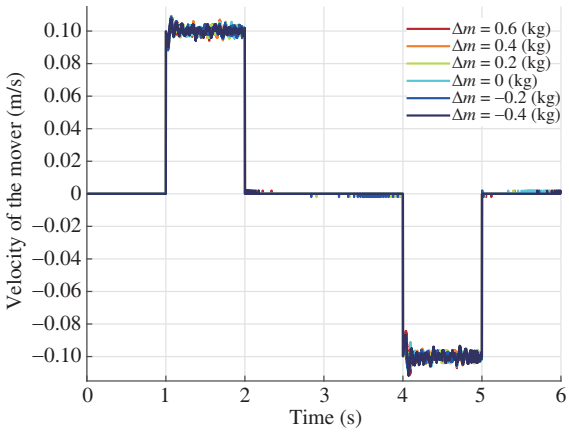

Figure 6 (Color online) The velocities of the mover for various load masses (26).

presented to estimate the system state and the total disturbance containing the uncertainty of control input. Based on the estimations from ESO and the sign of control input gain, the control input is generated by a designed dynamical system which forces the actual input to track the ideal input. Moreover, for a wide class of nonlinear uncertainties, the closed-loop transient performance of the proposed ADRC is investigated. The theoretical results illustrate that the tracking and estimating errors, as well as the difference between the actual and ideal control inputs, can be sufficiently small by tuning the parameter of ESO. Finally, the simulations of a single-link robotic manipulator system and the experiments of a PMLSM servo system are presented, which illustrates the effectiveness of the proposed ADRC.

Acknowledgements This work was supported by National Natural Science Foundations of China (Grant Nos. 62003202, 61973202, 61903085), Fundamental Research Funds for the Central Universities (Grant No. GK202003008), National Key R & D Program of China (Grant No. 2018YFA0703800), Guangdong Basic and Applied Basic Research Foundation (Grant No. 2019A1515111070), China Postdoctoral Science Foundation (Grant No. 2020M672965), and State Key Laboratory of Synthetical Automation for Process Industries and the National Center for Mathematics and Interdisciplinary Sciences, Chinese Academy of Sciences.

References

1 Gao Z. On the centrality of disturbance rejection in automatic control. ISA Trans, 2014, 53: 850–857
2 Zhao C, Guo L. PID controller design for second order nonlinear uncertain systems. Sci China Inf Sci, 2017, 60: 022201
3 Liu K Z, Yao Y. Robust Control. New York: Wiley, 2016
4 Liu L. Analysis and Design of Sliding Mode Control Systems. Beijing: Science Press, 2017
5 Li S, Yang J, Chen W H, et al. Disturbance Observer-Based Control: Methods and Applicaitons. Boca Raton: CRC Press, 2014
6 Sun J, Yang J, Zheng W X, et al. GPIO-based robust control of nonlinear uncertain systems under time-varying disturbance with application to DC-DC converter. IEEE Trans Circ Syst II, 2016, 63: 1074–1078
7 Liu R J, She J H, Wu M, et al. Robust disturbance rejection for a fractional-order system based on equivalent-input-disturbance approach. Sci China Inf Sci, 2018, 61: 070222
8 Han J. From PID to active disturbance rejection control. IEEE Trans Ind Electron, 2009, 56: 900–906
9 Chen S, Bai W Y, Hu Y, et al. On the conceptualization of total disturbance and its profound implications. Sci China Inf Sci, 2020, 63: 129201
10 Yuan Y, Cheng L, Wang Z D, et al. Position tracking and attitude control for quadrotors via active disturbance rejection control method. Sci China Inf Sci, 2019, 62: 010201
11 Sun J, Pu Z, Yi J. Conditional disturbance negation based active disturbance rejection control for hypersonic vehicles. Control Eng Practice, 2019, 84: 159–171
12 Su J, Ma H, Qiu W, et al. Task-independent robotic uncalibrated hand-eye coordination based on the extended state observer. IEEE Trans Syst Man Cybern B, 2004, 34: 1917–1922
13 Texas Instruments. Technical Reference Manual, TMS320F28069M, TMS320F28068M InstaSPINTMMOTION Software. Literature Number: SPRUHJ0A, 2013
14 Madonski R, Stanković M, Shao S, et al. Active disturbance rejection control of torsional plant with unknown frequency harmonic disturbance. Control Eng Practice, 2020, 100: 104413
15 Chen Z, Qin B, Sun M, et al. Q-learning-based parameters adaptive algorithm for active disturbance rejection control and its application to ship course control. Neurocomputing, 2020, 408: 51–63
16 Xia Y, Dai L, Fu M, et al. Application of active disturbance rejection control in tank gun control system. J Franklin Institute, 2014, 351: 2299–2314
17 Sun L, Shen J, Hua Q, et al. Data-driven oxygen excess ratio control for proton exchange membrane fuel cell. Appl Energy, 2018, 231: 866–875
18 Sun L, Jin Y, You F. Active disturbance rejection temperature control of open-cathode proton exchange membrane fuel cell. Appl Energy, 2020, 261: 114381

19 Yang X, Huang Y. Capabilities of extended state observer for estimating uncertainties. In: Proceedings of the 2009 American Control Conference, St Louis, 2009. 3700–3705
20 Guo B Z, Zhao Z L. On the convergence of an extended state observer for nonlinear systems with uncertainty. Syst Control Lett, 2011, 60: 420–430
21 Zheng Q, Chen Z, Gao Z. A practical approach to disturbance decoupling control. Control Eng Practice, 2009, 17: 1016–1025
22 Li J, Xia Y, Qi X, et al. Robust absolute stability analysis for interval nonlinear active disturbance rejection based control system. ISA Trans, 2017, 69: 122–130
23 Xue W, Huang Y. Performance analysis of 2-DOF tracking control for a class of nonlinear uncertain systems with discontinuous disturbances. Int J Robust Nonlin Control, 2018, 28: 1456–1473
24 Shao S, Gao Z. On the conditions of exponential stability in active disturbance rejection control based on singular perturbation analysis. Int J Control, 2017, 90: 2085–2097
25 Zhao Z L, Guo B Z. A novel extended state observer for output tracking of MIMO systems with mismatched uncertainty. IEEE Trans Automat Contr, 2018, 63: 211–218
26 Chen S, Xue W, Huang Y. On active disturbance rejection control for nonlinear systems with multiple uncertainties and nonlinear measurement. Int J Robust Nonlin Control, 2020, 30: 3411–3435
27 Chen S, Huang Y, Zhao Z L. The necessary and sufficient condition for the uncertain control gain in active disturbance rejection control. 2020. ArXiv:2006.11731
28 Lee J, Mukherjee R, Khalil H K. Output feedback performance recovery in the presence of uncertainties. Syst Control Lett, 2016, 90: 31–37
29 Yi B, Lin S, Yang B, et al. Performance recovery of a class of uncertain non-affine systems with unmodelled dynamics: an indirect dynamic inversion method. Int J Control, 2018, 91: 266–284
30 Ran M, Wang Q, Dong C. Active disturbance rejection control for uncertain nonaffine-in-control nonlinear systems. IEEE Trans Automat Contr, 2017, 62: 5830–5836
31 Yoo D, Yau S S T, Gao Z. Optimal fast tracking observer bandwidth of the linear extended state observer. Int J Control, 2007, 80: 102–111
32 Zhao Z L, Jiang Z P. Semi-global finite-time output-feedback stabilization with an application to robotics. IEEE Trans Ind Electron, 2019, 66: 3148–3156
33 Ting C S, Lieu J F, Liu C S, et al. An adaptive FNN control design of PMLSM in stationary reference frame. J Control Autom Electr Syst, 2016, 27: 391–405

Appendix A Proof of Theorem 1

The proof consists of the following four steps:

(1) The analysis for the closed-loop form of the error system;

(2) The analysis for the bounds of uncertain terms in the closed-loop system;

(3) The analysis for the trajectories of the closed-loop system in $[t_0, t_u)$;

(4) The analysis for the trajectories of the closed-loop system in $[t_u, \infty)$.

Step 1. The analysis for the closed-loop form of the error systems.

Let the tracking and estimating errors and the difference between the actual and ideal inputs be $e(t) = x(t) - x^*(t)$, $\xi(t) = T_1^{-1}(x_e(t) - \hat{x}_e(t))$, $\delta_u(t) = u(t) - u^*(t)$, where T_1 is a diagonal matrix with the i-th diagonal element $T_1(i,i) = \omega_o^{i-n-1}$.

Next, we analyze the dynamics of (e, ξ, δ_u). According to the ideal control input (10), the system (1) can be rewritten as

$$\begin{aligned}\dot{x}(t) &= Ax(t) + B(b(x,t)u(t) + f(x,t) - b(x,t)u^*(t) + b(x,t)u^*(t))\\ &= Ax(t) - BK^{\mathrm{T}}(x(t) - \bar{r}(t)) + Br^{(n)}(t) + Bb\delta_u(t).\end{aligned} \tag{A1}$$

According to (9) and the definition of A_K, the dynamics of $e(t)$ is shown as follows:

$$\dot{e}(t) = A_K e(t) + Bb\delta_u(t). \tag{A2}$$

From (5), (7) and the definition of A_ϕ (16), the dynamics of ξ can be obtained as follows:

$$\dot{\xi}(t) = \omega_o A_\phi \xi(t) + B_f \dot{x}_{n+1}(t). \tag{A3}$$

By (13), the dynamics of δ_u can be calculated as

$$\begin{aligned}\dot{\delta}_u(t) &= -\mathrm{sgn}(b)\lambda(\hat{x}_{n+1}(t) + K^{\mathrm{T}}(\hat{x}(t) - \bar{r}(t)) - r^{(n)}(t)) - \dot{u}^*(t)\\ &= -|b(x,t)|\lambda\delta_u(t) + \mathrm{sgn}(b)\lambda K_e^{\mathrm{T}} T_1 \xi(t) - \dot{u}^*(t),\end{aligned} \tag{A4}$$

where $K_e = [K^{\mathrm{T}}\ 1]^{\mathrm{T}}$.

Based on (A2)–(A4), the closed-loop system is presented as follows:

$$\begin{cases}\dot{e}(t) = Ae(t) + B\Gamma_{e0}(e,t),\\ \dot{\xi}(t) = \omega_o A_\phi \xi(t) + B_f \Gamma_{\xi 0}(e,t), & t \in [t_0, t_u),\\ \dot{\delta}_u(t) = -|b(x,t)|\lambda\delta_u(t) + \Gamma_{\delta_u 0}(e,\xi,\omega_o,\lambda,t),\end{cases} \tag{A5}$$

$$\begin{cases}\dot{e}(t) = A_K e(t) + B\Gamma_{e1}(e,\delta_u,t),\\ \dot{\xi}(t) = \omega_o A_\phi \xi(t) + B_f \Gamma_{\xi 1}(e,\xi,\delta_u,\omega_o,\lambda,t), & t \in [t_u, \infty),\\ \dot{\delta}_u(t) = -|b(x,t)|\lambda\delta_u(t) + \Gamma_{\delta_u 1}(e,\xi,\delta_u,\omega_o,\lambda,t),\end{cases} \tag{A6}$$

where A_ϕ is defined in (16) and

$$\begin{cases}\Gamma_{e0}=f(e+x^*,t)+K^{\mathrm{T}}(x^*-\bar{r})-r^{(n)},\quad \Gamma_{e1}=b\delta_u,\\ \Gamma_{\xi 0}=\frac{\partial f}{\partial x}(A(e+x^*)+Bf(e+x^*,t))+\frac{\partial f}{\partial t},\\ \Gamma_{\xi 1}=(-\lambda b|b|+\frac{\partial b}{\partial x}(A_Ke+Bb\delta_u+\dot{x}^*)+\frac{\partial b}{\partial t})\delta_u+|b|\lambda K_{\mathrm{e}}^{\mathrm{T}}T_1\xi+\frac{\partial f}{\partial x}(A_Ke+Bb\delta_u+\dot{x}^*)\\ \qquad +(\frac{\partial b}{\partial x}(A_Ke+Bb\delta_u+\dot{x}^*)+\frac{\partial b}{\partial t})(-f(e+x^*,t)-K^{\mathrm{T}}(e+x^*-\bar{r})+r^{(n)})/b+\frac{\partial f}{\partial t},\\ \Gamma_{\delta_u 0}=(\frac{\partial f}{\partial x}(A(e+x^*)+Bf(e+x^*,t))+\frac{\partial f}{\partial t}+K^{\mathrm{T}}(A(e+x^*)+Bf(e+x^*,t)-\dot{\bar{r}})-r^{(n+1)})/b\\ \qquad +(-f(e+x^*,t)-K^{\mathrm{T}}(e+x^*-\bar{r})+r^{(n)})(\frac{\partial b}{\partial x}(A(e+x^*)+Bf(e+x^*,t))+\frac{\partial b}{\partial t})/b^2+\mathrm{sgn}(b)\lambda K_{\mathrm{e}}^{\mathrm{T}}T_1\xi,\\ \Gamma_{\delta_u 1}=(\frac{\partial f}{\partial x}(A_Ke+Bb\delta_u+\dot{x}^*)+\frac{\partial f}{\partial t}+\frac{K^{\mathrm{T}}(A_Ke+Bb\delta_u+\dot{x}^*-\dot{\bar{r}})-r^{(n+1)})}{b}+\mathrm{sgn}(b)\lambda K_{\mathrm{e}}^{\mathrm{T}}T_1\xi\\ \qquad +(-f(e+x^*,t)-K^{\mathrm{T}}(e+x^*-\bar{r})+r^{(n)})(\frac{\partial b}{\partial x}(A_Ke+Bb\delta_u+\dot{x}^*)+\frac{\partial b}{\partial t})/b^2.\end{cases}\tag{A7}$$

Because the matrices A_K and A_ϕ are Hurwitz, there exist positive definite matrices P_K and P_ϕ such that $A_K^{\mathrm{T}}P_K+P_KA_K=-I$ and $A_\phi^{\mathrm{T}}P_\phi+P_\phi A_\phi=-I$.

Step 2. The analysis for the bounds of uncertain terms $(\Gamma_{e0},\Gamma_{\xi 0},\Gamma_{\delta_u 0},\Gamma_{e1},\Gamma_{\xi 1},\Gamma_{\delta_u 1})$.

Owing to Assumption 1 and (9), there exists a positive constant M_{x^*} such that $\sup_{t\geqslant t_0}\{\|x^*(t)\|,\|\dot{x}^*(t)\|\}\leqslant M_{x^*}$. With the combination of (A7) and Assumptions 1 and 2, the bounds of Γ_{e0}, $\Gamma_{\xi 0}$, $\Gamma_{\delta_u 0}$, Γ_{e1}, $\Gamma_{\xi 1}$ and $\Gamma_{\delta_u 1}$ can be obtained. To simplify the expression of these boundaries, we introduce the non-decreasing function $\Psi(a)\triangleq\sup_{\|x\|\leqslant a}\{\psi_f(x),\psi_{\bar{r}}(x),1/\psi_{\underline{b}}(x)\}$.

Considering any given positives ρ_e, ρ_ξ, ρ_{δ_u} and ω_o^*, for any $e\in\{e|\ \|e\|\leqslant\rho_e\}$, $\xi\in\{\xi|\ \|\xi\|\leqslant\rho_\xi\}$, $\delta_u\in\{\delta_u|\ |\delta_u|\leqslant\rho_{\delta_u}\}$ and $\omega_o\in\{\omega_o|\ \omega_o\geqslant\omega_o^*\}$, there is

$$\begin{cases}|\Gamma_{e0}|\leqslant\pi_{e0}(\rho_e),\quad |\Gamma_{e1}|\leqslant\pi_{e1}(\rho_e)|\delta_u|,\\ |\Gamma_{\xi 0}|\leqslant\pi_{\xi 0}(\rho_e),\quad |\Gamma_{\xi 1}|\leqslant\pi_{\xi 1}(\rho_e)+(\lambda+1)\pi_{\delta_u}(\rho_e,\rho_{\delta_u})+\pi_\omega(\omega_o^*)\Psi(\rho_e+M_{x^*})\lambda\|\xi\|,\\ |\Gamma_{\delta_u 0}|\leqslant\pi_{\delta_u 0}(\rho_e)+\pi_\omega(\omega_o^*)\lambda\|\xi\|,\quad |\Gamma_{\delta_u 1}|\leqslant\pi_{\delta_u 1}(\rho_e,\rho_{\delta_u})+\pi_\omega(\omega_o^*)\lambda\|\xi\|,\end{cases}\tag{A8}$$

where $\pi_{e0}(\rho_e)\triangleq\Psi(\rho_e+M_{x^*})+\|K\|(M_{x^*}+nM_r)+M_r$, $\pi_{e1}(\rho_e)\triangleq\Psi(\rho_e+M_{x^*})$, $\pi_{\xi 0}(\rho_e)\triangleq\Psi(\rho_e+M_{x^*})(1+\|A\|(\rho_e+M_{x^*})+\Psi(\rho_e+M_{x^*}))$, $\pi_{\xi 1}(\rho_e)\triangleq\Psi(\rho_e+M_{x^*})(\|A_K\|\rho_e+M_{x^*}+1)(1+\Psi(\rho_e+M_{x^*})(\Psi(\rho_e+M_{x^*})+\|K\|(\rho_e+M_{x^*}+nM_r)+M_r))$, $\pi_{\delta_u}(\rho_e,\rho_{\delta_u})\triangleq\Psi^2(\rho_e+M_{x^*})\rho_{\delta_u}^2+(2\Psi^2(\rho_e+M_{x^*})+\Psi(\rho_e+M_{x^*})(\|A_K\|\rho_e+M_{x^*}+1))(1+\Psi(\rho_e+M_{x^*})(\Psi(\rho_e+M_{x^*})+\|K\|(\rho_e+M_{x^*}+nM_r)+M_r))(\rho_{\delta_u}+1)$, $\pi_\omega(\omega_o)\triangleq\|K_e\|T_1(\omega_o)$, $\pi_{\delta_u 0}\triangleq(\Psi(\rho_e+M_{x^*})(1+\|A\|(\rho_e+M_{x^*}))+\|K\|(\|A\|(\rho_e+M_{x^*})+\Psi(\rho_e+M_{x^*})-nM_r)+M_r)\Psi(\rho_e+M_{x^*})+\Psi^3(\rho_e+M_{x^*})(\Psi(\rho_e+M_{x^*})+\|K\|(\rho_e+M_{x^*}+nM_r)+M_r)(1+\|A\|(\rho_e+M_{x^*})+\Psi(\rho_e+M_{x^*}))$, and $\pi_{\delta_u 1}\triangleq(\Psi(\rho_e+M_{x^*})(\|A_K\|\rho_e+\Psi(\rho_e+M_{x^*})\rho_{\delta_u}+M_{x^*}+1)+\|K\|(\|A_K\|\rho_e+\Psi(\rho_e+M_{x^*})\rho_{\delta_u}+M_{x^*}+nM_r)+M_r)\Psi(\rho_e+M_{x^*})+(\Psi(\rho_e+M_{x^*})+\|K\|(\rho_e+M_{x^*}+nM_r)+M_r)(\|A_K\|\rho_e+\Psi(\rho_e+M_{x^*})\rho_{\delta_u}+M_{x^*}+1)\Psi^3(\rho_e+M_{x^*})$. The functions $\pi_{e0}(a)$, $\pi_{e1}(a)$, $\pi_{\xi 0}(a)$, $\pi_{\xi 1}(a)$, $\pi_{\delta_u}(a,b)$, $\pi_{\delta_u 0}(a)$ and $\pi_{\delta_u 1}(a,b)$ are non-decreasing with respect to the variables a and b. The function $\pi_\omega(a)$ is non-increasing with respect to the variable a. More importantly, Eq. (A8) shows that the bounds of $(\Gamma_{e0},\Gamma_{\xi 0},\Gamma_{\delta_u 0},\Gamma_{e1},\Gamma_{\xi 1},\Gamma_{\delta_u 1})$ depend on the bounds of (e,ξ,δ_u) and the lower bound of ω_o.

Step 3. The analysis for the trajectories of the closed-loop system in $[t_0,t_u)$.

Owing to the definition of t_u and Assumption 3, it can be deduced that $\lim_{\omega_o\to\infty}t_u=t_0$. According to the dynamics (A5), there exists a positive ω_1 satisfying $\omega_1\geqslant\max\{1,\rho_0\}$ such that t_u-t_0 is suitably small and $\|e(t)\|\leqslant\eta_{e1}(\omega_1)$ for $t\in[t_0,t_u)$ and $\omega_o\geqslant\omega_1$, where $\eta_{e1}(\omega_1)$ is a positive constant dependent on ω_1. Thus, it can be deduced from (A5) that

$$\sup_{t_0\leqslant t\leqslant t_u}\|e(t)\|\leqslant 4nc_{\phi 2}(\|A\|\eta_{e1}+\pi_{e0}(\eta_{e1}))\frac{\ln\omega_o}{\sqrt{\lambda}},\tag{A9}$$

where $c_{\phi 2}$ is presented in (16).

Let $V_\phi(t)=\xi^{\mathrm{T}}(t)P_\phi\xi(t)$ and $V_u(t)=\delta_u^2(t)/2$. Let $c_{\phi 1}$ and $c_{\phi 2}$ be the minimal and maximal eigenvalues of P_ϕ, respectively. Then, we define a non-increasing function: $\Psi_{\underline{b}}(a)\triangleq\inf_{\|x\|\leqslant a}\psi_{\underline{b}}(x)$. According to Assumption 2, there exists a positive constant $M(a)$ such that $\Psi_{\underline{b}}(a)>M(a)>0$ for any given $a\geqslant 0$. Hence let the positive constant $\eta_{\underline{b}1}\triangleq\Psi_{\underline{b}}(\eta_{e1}+M_{x^*})$.

Based on (A5), the dynamics of $\sqrt{V_\phi(t)}$ and $\sqrt{V_u(t)}$ for $t\in[t_0,t_u)$ satisfies

$$\begin{cases}\dfrac{\mathrm{d}\sqrt{V_\phi(t)}}{\mathrm{d}t}=\dfrac{-\omega_o\|\xi\|^2+2\xi^{\mathrm{T}}P_\phi B_f\Gamma_{\xi 0}}{2\sqrt{V_\phi}}\leqslant-\dfrac{\omega_o}{2c_{\phi 2}}\sqrt{V_\phi(t)}+\dfrac{\|P_\phi\|\pi_{\xi 0}(\eta_{e1})}{\sqrt{c_{\phi 1}}},\\ \dfrac{\mathrm{d}\sqrt{V_u(t)}}{\mathrm{d}t}=\dfrac{-|b|\lambda|\delta_u|^2+\delta_u\Gamma_{\delta_u 0}}{2\sqrt{V_u}}\leqslant-\eta_{\underline{b}1}\lambda\sqrt{V_u(t)}+\dfrac{\sqrt{2}\pi_{\delta_u 0}(\eta_{e1})+\sqrt{2}\pi_\omega\lambda\|\xi(t)\|}{2}.\end{cases}\tag{A10}$$

Owing to Gronwall lemma, Eq. (A10) implies that $\sqrt{V_\phi(t)}$ has the following bound:

$$\sqrt{V_\phi(t)}\leqslant\frac{2c_{\phi 2}\|P_\phi\|\pi_{\xi 0}(\eta_{e1})}{\sqrt{c_{\phi 1}}\omega_o}+\sqrt{V_\phi(t_0)}\mathrm{e}^{-\frac{\omega_o(t-t_0)}{2c_{\phi 2}}},\quad t\in[t_0,t_u].\tag{A11}$$

Based on Gronwall lemma, (A10), and (A11), the bound of $\sqrt{V_u(t)}$ is given as follows:

$$\begin{aligned}\sqrt{V_u(t)}&\leqslant\frac{\sqrt{2}\pi_{\delta_u 0}(\eta_{e1})}{2\eta_{\underline{b}1}\lambda}+\sqrt{V_u(t_0)}\mathrm{e}^{-\eta_{\underline{b}1}\lambda(t-t_0)}+\int_{t_0}^t\mathrm{e}^{-\eta_{\underline{b}1}\lambda(t-s)}\sqrt{2}\pi_\omega\lambda\|\xi(s)\|\mathrm{d}s\\ &\leqslant\frac{\sqrt{2}\pi_{\delta_u 0}(\eta_{e1})}{2\eta_{\underline{b}1}\lambda}+\frac{\sqrt{2}\pi_\omega c_{\phi 2}\|P_\phi\|\pi_{\xi 0}(\eta_{e1})}{c_{\phi 1}\eta_{\underline{b}1}\omega_o}+\sqrt{V_u(t_0)}\mathrm{e}^{-\eta_{\underline{b}1}\lambda(t-t_0)}\end{aligned}$$

$$+\frac{\sqrt{2}\pi_\omega\lambda\sqrt{V_\phi(t_0)}}{\sqrt{c_{\phi 1}}(\frac{\omega_o}{2c_{\phi 2}}-\eta_{\underline{b}1}\lambda)}\mathrm{e}^{-\eta_{\underline{b}1}\lambda(t-t_0)}\left(1-\mathrm{e}^{-(\frac{\omega_o}{2c_{\phi 2}}-\eta_{\underline{b}1}\lambda)(t-t_0)}\right). \tag{A12}$$

We consider the case that $\rho_0>\frac{1}{\omega_o}$. Notice that $\sqrt{V_\phi(t_0)}\leqslant n\sqrt{c_{\phi 2}}\omega_o^{n-1}\rho_0^{n-1}$. Recalling the definition of t_u in (16), the following equations hold for $\frac{\omega_o}{\lambda}\geqslant 1$ and $\lambda\geqslant\frac{1}{4\eta_{\underline{b}1}^2c_{\phi 2}^2}$:

$$\sqrt{V_\phi(t_0)}\mathrm{e}^{-\frac{\omega_o(t_u-t_0)}{2c_{\phi 2}}}=\sqrt{V_\phi(t_0)}\mathrm{e}^{-\frac{n\omega_o}{\sqrt{\lambda}}\ln(\omega_o\rho_0)}\leqslant\frac{n\sqrt{c_{\phi 2}}}{\omega_o\rho_0},\quad \mathrm{e}^{-\eta_{\underline{b}1}\lambda(t_u-t_0)}=\mathrm{e}^{-2nc_{\phi 2}\eta_{\underline{b}1}\sqrt{\lambda}\ln(\omega_o\rho_0)}\leqslant\frac{1}{\rho_0^n\omega_o^n}. \tag{A13}$$

Based on (A11)–(A13), it can be deduced that

$$\begin{cases}\sqrt{V_\phi(t_u)}\leqslant\eta_{V_\phi 1}(\omega_2)\triangleq\dfrac{2c_{\phi 2}\|P_\phi\|\pi_{\xi 0}(\eta_{e1})}{\sqrt{c_{\phi 1}}\omega_2}+\dfrac{n\sqrt{c_{\phi 2}}}{\rho_0\omega_2},\\ \sqrt{V_u(t_u)}\leqslant\eta_{V_u 1}(\omega_2,\lambda_2)\triangleq\dfrac{\sqrt{2}\pi_{\delta_u 0}(\eta_{e1})}{2\eta_{\underline{b}1}\lambda_2}+\dfrac{\sqrt{2}\pi_\omega(\omega_2)c_{\phi 2}\|P_\phi\|\pi_{\xi 0}(\eta_{e1})}{c_{\phi 1}\eta_{\underline{b}1}\omega_2}+\dfrac{\sqrt{V_u(t_0)}}{\omega_2^n\rho_0^n}+\dfrac{\sqrt{2}\pi_\omega(\omega_2)n\sqrt{c_{\phi 2}}}{\sqrt{c_{\phi 1}}\eta_{\underline{b}1}\rho_0\omega_2},\end{cases}$$

for any $\omega_o\geqslant\omega_2$, $\lambda\geqslant\lambda_2$ and $\frac{\omega_o}{\lambda}\geqslant\tau_2$, where $\omega_2=\max\{\lambda_2\tau_2,\omega_1\}$, $\lambda_2=\frac{1}{4\eta_{\underline{b}1}^2c_{\phi 2}^2}$ and $\tau_2=\max\{1,4\eta_{\underline{b}1}c_{\phi 2}\}$.

If $\rho_0\leqslant\frac{1}{\omega_o}$, then $t_u=t_0$. Moreover, it can be proved that $\|e(t_u)\|$, $\sqrt{V_\phi(t_u)}$ and $\sqrt{V_u(t_u)}$ are bounded for any $\omega_o\geqslant\omega_2$. Without loss of generality, for $\rho_0\leqslant\frac{1}{\omega_o}$, let η_{e1}, $\eta_{V_\phi 1}$ and $\eta_{V_u 1}$ denote the bounds of $\|e(t_u)\|$, $\sqrt{V_\phi(t_u)}$ and $\sqrt{V_u(t_u)}$, respectively. The similar derivatives as the case that $\rho_0>\frac{1}{\omega_o}$ can be made. Thus, in the next step, the analysis for the case that $\rho_0>\frac{1}{\omega_o}$ is presented.

Step 4. The analysis for the trajectories of the closed-loop system in $[t_u,\infty)$.

Owing to the dynamics (13), (A5), and (A6), (e,ξ,u) are continuous at t_u. Let $V_K(t)=\mathrm{e}^{\mathrm{T}}(t)P_Ke(t)$, c_{k1} and c_{k2} be the minimal and maximum eigenvalues of P_K, respectively. Then the following constants are introduced.

$$\begin{cases}\eta_{V_K 2}\triangleq\sqrt{c_{k2}}\max\{\eta_{e1},2\|P_K\|\pi_{e1}(\eta_{e2})\eta_{\delta_u 2}\},\ \eta_{V_\phi 2}\triangleq\eta_{V_\phi 1},\ \eta_{V_u 2}\triangleq\max\left\{\eta_{V_u 1},\dfrac{2\pi_\omega(\omega_2)\eta_{\xi 2}}{\eta_{\underline{b}2}}\right\},\\ \eta_{e2}\triangleq\dfrac{\eta_{V_K 1}}{\sqrt{c_{k1}}},\quad \eta_{\xi 2}\triangleq\dfrac{\eta_{V2}}{\sqrt{c_{21}}},\quad \eta_{\delta_u 2}\triangleq\dfrac{\eta_{V2}}{\sqrt{c_{21}}},\quad \eta_{\underline{b}2}\triangleq\Psi_{\underline{b}}(\eta_{e2}+M_{x^*}).\end{cases} \tag{A14}$$

Then we will prove that there exist positives ω_3, λ_3 and τ_3 such that $e(t),\xi(t),\delta_u(t)$ stay in a bounded set $\Omega_1\triangleq\{(e,\xi,\delta_u)\mid\sqrt{V_K}\leqslant\eta_{V_K 2},\ \sqrt{V_\phi}\leqslant\eta_{V_\phi 2},\ \sqrt{V_u}\leqslant\eta_{V_u 2}\}$ for $\omega_o\geqslant\omega_3$, $\lambda\geqslant\lambda_3$, $\frac{\omega_o}{\lambda}\geqslant\tau_3$ and $t\geqslant t_u$. The proof consists of the following three steps.

(S1) We assume that there exists a positive t^* satisfying $t^*\in[t_u,\infty)$ such that $\sqrt{V_\phi(t^*)}=\eta_{V_\phi 2}$. Besides, $\sqrt{V_\phi(t)}\leqslant\eta_{V_\phi 2}$, $\sqrt{V_K(t)}\leqslant\eta_{V_K 2}$ and $\sqrt{V_{\delta_u}(t)}\leqslant\eta_{V_u 2}$ for $t\in[t_u,t^*]$. Then it can be deduced that $\|e(t)\|\leqslant\eta_{e2}$, $\|\xi(t)\|\leqslant\eta_{\xi 2}$ and $|\delta_u(t)|\leqslant\eta_{\delta_u 2}$ for $t\in[t_u,t^*]$. Owing to the dynamics (A6) and the bound of $\Gamma_{\xi 1}$ (A8), the derivative of $\sqrt{V_\phi(t^*)}$ satisfies

$$\frac{\mathrm{d}\sqrt{V_\phi(t^*)}}{\mathrm{d}t}\leqslant-\frac{\omega_o\eta_{V_\phi 2}}{2c_{\phi 2}}+\frac{\|P_\phi\|(\pi_{\xi 1}(\eta_{e2})+(\lambda+1)\pi_{\delta_u}(\eta_{e2},\eta_{\delta_u 2})+\pi_\omega(\omega_o)\Psi(\eta_{e2}+M_{x^*})\lambda\eta_{\xi 2})}{\sqrt{c_{\phi 1}}}. \tag{A15}$$

By selecting $\omega_3=\max\{\omega_2,(6c_{\phi 2}\|P_\phi\|(\pi_{\xi 1}(\eta_{e2})+\pi_{\delta_u}(\eta_{e2},\eta_{\delta_u 2})))/(\eta_{V_\phi 2}\sqrt{c_{\phi 1}})\}$ and $\tau_3=(6c_{\phi 2}\|P_\phi\|(\pi_\omega(\omega_2)\Psi(\eta_{e2}+M_{x^*})\eta_{\xi 2}+\pi_{\delta_u}(\eta_{e2},\eta_{\delta_u 2})))/(\eta_{V_\phi 2}\sqrt{c_{\phi 1}})$, the inequality (A15) directly implies that $\frac{\mathrm{d}\sqrt{V_\phi(t^*)}}{\mathrm{d}t}<0$ for (ω_o,λ) satisfying $\omega_o\geqslant\omega_3$ and $\frac{\omega_o}{\lambda}\geqslant\tau_3$.

(S2) We assume that there exists a positive t^* satisfying $t^*\in[t_u,\infty)$ such that $\sqrt{V_u(t^*)}=\eta_{V_u 2}$. Besides, $\sqrt{V_u(t)}\leqslant\eta_{V_u 2}$, $\sqrt{V_K(t)}\leqslant\eta_{V_K 2}$ and $\sqrt{V_\phi(t)}\leqslant\eta_{V_\phi 2}$ for $t\in[t_u,t^*]$. Hence $\|e(t)\|\leqslant\eta_{e2}$, $\|\xi(t)\|\leqslant\eta_{\xi 2}$, $|\delta_u(t)|\leqslant\eta_{\delta_u 2}$ and $|b(x,t)|\geqslant\eta_{\underline{b}2}$ for $t\in[t_u,t^*]$. Based on (A6) and (A8), the derivative of $\sqrt{V_u(t^*)}$ satisfies that $\frac{\mathrm{d}\sqrt{V_u(t^*)}}{\mathrm{d}t}\leqslant-\eta_{\underline{b}2}\eta_{V_u 2}\lambda+\frac{\sqrt{2}}{2}(\pi_{\delta_u 1}(\eta_{e2},\eta_{\delta_u 2})+\pi_\omega\lambda\eta_{\xi 2})$. Owing to the definition of $\eta_{V_u 2}$ in (A14), we have $-\frac{\eta_{\underline{b}2}\eta_{V_u 2}}{2}+\pi_\omega(\omega_2)\eta_{\xi 2}\leqslant 0$ for any $\omega_o\geqslant\omega_3$. By choosing $\lambda_3=\frac{2\sqrt{2}\pi_{\delta_u 1}(\eta_{e2},\eta_{\delta_u 2})}{\eta_{\underline{b}2}\eta_{V_u 2}}$, it can be verified that $\frac{\mathrm{d}\sqrt{V_u(t^*)}}{\mathrm{d}t}<0$ for $\omega_o\geqslant\omega_3$ and $\lambda\geqslant\lambda_3$.

(S3) We assume that there exists a positive t^* satisfying $t^*\in[t_u,\infty)$ such that $\sqrt{V_K(t^*)}=\eta_{V_K 2}$. Besides, $\sqrt{V_K(t)}\leqslant\eta_{V_K 2}$, $\sqrt{V_\phi(t)}\leqslant\eta_{V_\phi 2}$ and $\sqrt{V_u(t)}\leqslant\eta_{V_u 2}$ for $t\in[t_u,t^*]$. Hence $\|e(t)\|\leqslant\eta_{e2}$, $\|\xi(t)\|\leqslant\eta_{\xi 2}$ and $|\delta_u(t)|\leqslant\eta_{\delta_u 2}$ for $t\in[t_u,t^*]$. According to (A6), (A8) and (A14), the derivative of $\sqrt{V_K(t^*)}$ satisfies that $\frac{\mathrm{d}\sqrt{V_K(t^*)}}{\mathrm{d}t}\leqslant-\frac{\|e(t^*)\|}{2\sqrt{V_K(t^*)}}(\|e(t^*)\|-2\|P_K\|\pi_{e1}(\eta_{e2})\eta_{\delta_u 2})<0$.

Based on (S1)–(S3), it can be concluded that the variables $(e(t),\xi(t),\delta_u(t))$ stay in Ω_1 for any $\omega_o\geqslant\omega_3$, $\lambda\geqslant\lambda_3$ and $\frac{\omega_o}{\lambda}\geqslant\tau_3$. Next, we analyze the bounds of $\sqrt{V_K(t)}$, $\sqrt{V_\phi(t)}$ and $\sqrt{V_u(t)}$ for $t\geqslant t_u$.

Firstly, the bound of $\sqrt{V_\phi(t)}$ is studied. Owing to (A6) and (A8), for $t\geqslant t_u$, we have

$$\frac{\mathrm{d}\sqrt{V_\phi(t)}}{\mathrm{d}t}\leqslant-\frac{\omega_o}{2c_{\phi 2}}\sqrt{V_\phi(t)}+\frac{\|P_\phi\|(\pi_{\xi 1}(\eta_{e2})+(\lambda+1)\pi_{\delta_u}(\eta_{e2},\eta_{\delta_u 2})+\pi_\omega(\omega_o)\Psi(\eta_{e2}+M_{x^*})\lambda\eta_{\xi 2})}{\sqrt{c_{\phi 1}}}. \tag{A16}$$

Based on Gronwall lemma, $\sqrt{V_\phi(t)}$ has the following bound:

$$\sqrt{V_\phi(t)}\leqslant\eta_{V_\phi 2}\mathrm{e}^{-\frac{\omega_o(t-t_u)}{2c_{\phi 2}}}+\theta_{\phi 1}\frac{1}{\omega_o}+\theta_{\phi 2}\frac{\lambda}{\omega_o},\quad\forall t\in[t_u,\infty), \tag{A17}$$

for $\omega_o\geqslant\omega_3$, $\lambda\geqslant\lambda_3$ and $\frac{\omega_o}{\lambda}\geqslant\tau_3$, where $\theta_{\phi 1}=(\|P_\phi\|(\pi_{\xi 1}(\eta_{e2})+\pi_{\delta_u}(\eta_{e2},\eta_{\delta_u 2})))/\sqrt{c_{\phi 1}}$ and $\theta_{\phi 2}=(\|P_\phi\|(\pi_{\delta_u}(\eta_{e2},\eta_{\delta_u 2})+\pi_\omega(\omega_3)\Psi(\eta_{e2}+M_{x^*})\eta_{\xi 2}))/\sqrt{c_{\phi 1}}$.

Secondly, we analyze the bound of $\sqrt{V_u(t)}$. Owing to (A6), (A8) and (A17), for $t \geqslant t_u$, we have

$$\begin{aligned}\frac{\mathrm{d}\sqrt{V_u(t)}}{\mathrm{d}t} &\leqslant -\eta_{\underline{b}2}\lambda\sqrt{V_u(t)} + \frac{\sqrt{2}}{2}(\pi_{\delta_u 1}(\eta_{e2},\eta_{\delta_u 2}) + \pi_\omega\lambda\|\xi(t)\|)\\ &\leqslant -\eta_{\underline{b}2}\lambda\sqrt{V_u(t)} + \frac{\sqrt{2}}{2}\left(\pi_{\delta_u 1}(\eta_{e2},\eta_{\delta_u 2}) + \lambda\frac{\pi_\omega(\eta_{V_\phi 2}\mathrm{e}^{-\frac{\omega_o}{2c_{\phi 2}}(t-t_u)} + \theta_{\phi 1}\frac{1}{\omega_o} + \theta_{\phi 2}\frac{\lambda}{\omega_o})}{\sqrt{c_{\phi 1}}}\right).\end{aligned} \tag{A18}$$

Based on Gronwall lemma, the bound of $\sqrt{V_u(t)}$ is shown as follows:

$$\begin{aligned}\sqrt{V_u(t)} &\leqslant \eta_{V_u 2}\mathrm{e}^{-\eta_{\underline{b}2}\lambda(t-t_u)} + \theta_{u1}\frac{1}{\omega_o} + \theta_{u2}\frac{\lambda}{\omega_o} + \theta_{u3}\frac{1}{\lambda} + \theta_{u4}\int_{t_u}^{t}\mathrm{e}^{-\eta_{\underline{b}2}\lambda(t-s)}\mathrm{e}^{-\frac{\omega_o}{2c_{\phi 2}}(s-t_u)}\mathrm{d}s\\ &\leqslant \left(\eta_{V_u 2} + \frac{\theta_{u4}}{\eta_{\underline{b}2}\lambda_3}\right)\mathrm{e}^{-\eta_{\underline{b}2}\lambda(t-t_u)} + \theta_{u1}\frac{1}{\omega_o} + \theta_{u2}\frac{\lambda}{\omega_o} + \theta_{u3}\frac{1}{\lambda}, \quad \forall t\in[t_u,\infty),\end{aligned} \tag{A19}$$

for $\omega_o \geqslant \omega_3$, $\lambda \geqslant \lambda_3$ and $\frac{\omega_o}{\lambda} \geqslant \tau_4 \triangleq \max\{\tau_3, 4c_{\phi 2}\eta_{\underline{b}2}\}$, where $\theta_{u1} = \frac{\sqrt{2}\pi_\omega(\omega_3)\theta_{\phi 1}}{2\eta_{\underline{b}2}\sqrt{c_{\phi 1}}}$, $\theta_{u2} = \frac{\sqrt{2}\pi_\omega(\omega_3)\theta_{\phi 2}}{2\eta_{\underline{b}2}\sqrt{c_{\phi 1}}}$, $\theta_{u3} = \frac{\sqrt{2}\pi_{\delta_u 1}(\eta_{e2},\eta_{\delta_u 2})}{2\eta_{\underline{b}2}}$ and $\theta_{u4} = \frac{\sqrt{2}\pi_\omega(\omega_3)\eta_{V_\phi 2}}{2\eta_{\underline{b}2}\sqrt{c_{\phi 1}}}$.

Thirdly, the bound of $\sqrt{V_K(t)}$ is investigated. By defining $\tilde{t}_u = t_u + \frac{\ln\omega_o}{\eta_{\underline{b}2}\sqrt{\lambda}}$, it can be deduced from (A6) and (A9) that

$$\begin{cases}\sup\limits_{t_u\leqslant t\leqslant\tilde{t}_u}\sqrt{V_K(t)} \leqslant \sqrt{c_{k2}}\left(\|e(t_u)\| + (\|A_K\|\eta_{e2} + \pi_{e1}(\eta_{e2})\eta_{\delta_u 2})\frac{\ln\omega_o}{\eta_{\underline{b}2}\sqrt{\lambda}}\right) \leqslant \theta_e\frac{\ln\omega_o}{\sqrt{\lambda}},\\ \mathrm{e}^{-\eta_{\underline{b}2}\lambda(\tilde{t}_u - t_u)} = \dfrac{1}{\omega_o^{\sqrt{\lambda}}} \leqslant \dfrac{1}{\omega_o},\end{cases} \tag{A20}$$

for $\omega_o \geqslant \omega_3$, $\lambda \geqslant \lambda_4 \triangleq \max\{\lambda_3, 1\}$ and $\frac{\omega_o}{\lambda} \geqslant \tau_4$, where $\theta_e = 4\sqrt{c_{k2}}nc_{\phi 2}(\|A\|\eta_{e1} + \pi_{e0}(\eta_{e1})) + \frac{\sqrt{c_{k2}}\|A_K\|\eta_{e2} + \sqrt{c_{k2}}\pi_{e1}(\eta_{e2})\eta_{\delta_u 2}}{\eta_{\underline{b}2}}$. Then the bound of $\sqrt{V_K(t)}$ for $t \geqslant \tilde{t}_u$ is analyzed. According to (A6), (A8), (A19), and (A20), the dynamics of $\sqrt{V_K(t)}$ satisfies the following inequality for $t \geqslant \tilde{t}_u$.

$$\begin{aligned}\frac{\mathrm{d}\sqrt{V_K(t)}}{\mathrm{d}t} &\leqslant -\frac{\sqrt{V_K(t)}}{2c_{k2}} + \frac{\sqrt{2}\|P_K\|\pi_{e1}(\eta_{e2})}{\sqrt{c_{k1}}}\left(\left(\eta_{V_u 2} + \frac{\theta_{u4}}{\eta_{\underline{b}2}\lambda}\right)\mathrm{e}^{-\eta_{\underline{b}2}\lambda(t-t_u)} + \frac{\theta_{u1}}{\omega_o} + \frac{\theta_{u2}\lambda}{\omega_o} + \frac{\theta_{u3}}{\lambda}\right)\\ &\leqslant -\frac{\sqrt{V_K(t)}}{2c_{k2}} + \frac{\sqrt{2}\|P_K\|\pi_{e1}(\eta_{e2})}{\sqrt{c_{k1}}}\left(\left(\eta_{V_u 2} + \frac{\theta_{u4}}{\eta_{\underline{b}2}\lambda} + \theta_{u1}\right)\frac{1}{\omega_o} + \frac{\theta_{u2}\lambda}{\omega_o} + \frac{\theta_{u3}}{\lambda}\right),\end{aligned} \tag{A21}$$

for $\omega_o \geqslant \omega_3$, $\lambda \geqslant \lambda_4$ and $\frac{\omega_o}{\lambda} \geqslant \tau_4$. With the help of Gronwall lemma, we get the following bound of $\sqrt{V_K}$.

$$\sup_{t\geqslant\tilde{t}_u}\sqrt{V_K(t)} \leqslant \sqrt{V_K(\tilde{t}_u)} + \theta_{e1}\frac{1}{\omega_o} + \theta_{e2}\frac{\lambda}{\omega_o} + \theta_{e3}\frac{1}{\lambda} \leqslant \theta_e\frac{\ln\omega_o}{\sqrt{\lambda}} + \theta_{e1}\frac{1}{\omega_o} + \theta_{e2}\frac{\lambda}{\omega_o} + \theta_{e3}\frac{1}{\lambda}, \tag{A22}$$

for $\omega_o \geqslant \omega_3$, $\lambda \geqslant \lambda_4$, and $\frac{\omega_o}{\lambda} \geqslant \tau_4$, where $\theta_{e1} = 2\sqrt{2}c_{k2}\|P_K\|\pi_{e1}(\eta_{e2})(\eta_{V_u 2} + \frac{\theta_{u4}}{\eta_{\underline{b}2}\lambda_3} + \theta_{u1})/\sqrt{c_{k1}}$, $\theta_{e2} = 2\sqrt{2}c_{k2}\|P_K\|\pi_{e1}(\eta_{e2})\theta_{u2}$ $/\sqrt{c_{k1}}$ and $\theta_{e3} = 2\sqrt{2}c_{k2}\|P_K\|\pi_{e1}(\eta_{e2})\theta_{u3}/\sqrt{c_{k1}}$.

According to Assumption 3, there exists a positive ω_4 satisfying $\omega_4 \geqslant \omega_3$ such that $\lambda(\omega_o) \geqslant \lambda_4$ and $\frac{\omega_o}{\lambda(\omega_o)} \geqslant \tau_4$ for any $\omega_o \geqslant \omega_4$. Notice that $\frac{1}{\omega_o} \leqslant \frac{\lambda}{\omega_o}$ for $\lambda \geqslant \lambda_4 \geqslant 1$. With the combination of the bounds of $\sup_{t_0\leqslant t\leqslant t_u}\|e(t)\|$, $\sqrt{V_K(t)}$, $\sqrt{V_\phi(t)}$ and $\sqrt{V_u(t)}$, i.e., (A9), (A17), (A19), (A20) and (A22), we prove (17)–(19).